Contents list available at CBIORE journal website

International Journal of Renewable Energy Development

Journal homepage: https://ijred.cbiore.id

Research Article

Nickel-vanadium impregnated to hydrotalcite for hydrocracking of waste cooking oil

Lenny Marlinda[a], Sugeng Priyanto[b], Peri Oktiarmi[c], Maja Pranata Marbun[d], Aisha Andini Indira Dewi[a], Sudibyo[e], Indri Yati[f], Abdul Aziz[g], Reva Edra Nugraha[h], Muhammad Al Muttaqii[f*]

[a]*Department of Chemistry, Faculty of Science and Technology, University of Jambi, Jambi, 36361 Indonesia*

[b]*Department of Mechanical Engineering, State University of Jakarta, East Jakarta, 13220, Indonesia*

[c]*Department of Chemistry, Jambi State Senior High School 3, Jambi, 36124, Indonesia*

[d]*Department of Chemical Engineering, Faculty of Engineering, Sunan Bonang University, Tuban, 62314, Indonesia*

[e]*Research Center for Minerals Technology, National Research and Innovation Agency (BRIN-Indonesia), Lampung Selatan, 35361, Indonesia*

[f]*Research Center for Catalysis, National Research and Innovation Agency, South Tangerang, 15314, Indonesia*

[g]*Department of Chemistry, Institut Teknologi Sepuluh Nopember, Keputih, Sukolilo, Surabaya, 60111, Indonesia*

[h]*Department of Chemical Engineering, Faculty of Engineering, Universitas Pembangunan Nasional "Veteran" Jawa Timur, Surabaya, East Java, 60294, Indonesia*

Abstract. Hydrotalcite (HT) is a type of clay mineral belonging to the group of layered double hydroxides (LDHs) or anionic clays, which has a layered structure like brucite ($Mg(OH)_2$), but some of the divalent cations (such as Mg^{2+}) are replaced by trivalent cations (such as Al^{3+}). HT as a heterogeneous catalyst is particularly attractive because it is easy to separate and resistant to high temperatures. HT as a catalyst can be used in hydrocracking reaction to produce biofuel. Metal impregnation on HT is very promising to enhance catalytic activity especially with the bifunctional mechanism of catalyst. Ni-V metal impregnation has been successfully carried out on HTc using wet impregnation method which is indicated by the results of X-Ray Diffraction (XRD) which shows the emergence of typical peaks of both metals and HTc in 2θ = 35–70° for HTc, 2θ = 37.22° (NiO) and 37.35° (V_2O_5) regions, 2θ = 43.58° for NiO, 2θ = 61.26° (V) and 63.07° (Ini). Scanning Electron Microscopy-Energy Dispersive X-ray (SEM-EDX) show a shape that is consistent with the characteristics of HT, namely the shape of the particles layered overlapping each other. In addition, the particle size of HTc is quite small with a scale of 1 μm indicating a particle size of hundreds of nanometers. EDX mapping shows that Ni and V have been dispersed evenly on the HTc surface. Based on the results of N_2 adsorption-desorption isotherms, it shows that mesopores are formed which are characterized by hysteresis loops. Ni-V metal impregnation increases the surface area up to 19.915 m^2/g and the pore diameter up to 37,642 nm. The results of the Waste Cooking Oil (WCO) hydrocraking reaction show that Ni-V metal impregnation can reduce the carboxylic acid composition up to 67.81% and increase hydrocarbons up to 15% at 10% Ni-V/HTc 1:2.

Keywords: Hydrotalcite (HTc), Bifunctional catalyst, Waste Cooking Oil (WCO), Hydrocracking, Biofuel

@ The author(s). Published by CBIORE. This is an open access article under the CC BY-SA license (http://creativecommons.org/licenses/by-sa/4.0/).

Received: 11th Nov 2025; Revised: 18th January 2026; Accepted: 10th February 2026; Available online: 21st February 2026

1. Introduction

Hydrotalcite (HT) is a type of clay mineral belonging to the group of layered double hydroxides (LDHs) or anionic clays, which has a layered structure like brucite ($Mg(OH)_2$), but some of the divalent cations (such as Mg^{2+}) are replaced by trivalent cations (such as Al^{3+}). This replacement causes the layers to become positively charged, so that anions such as carbonate (CO_3^{2-}) and water are bound in the interlayer space to balance the charge (Lauermannová *et al*., 2020). This unique structure provides superior properties such as anion exchange capacity, high surface area, thermal stability, and strong alkaline properties after undergoing the calcination process. After calcination at temperatures around 400–600 °C, hydrotalcite will change into a mixture of metal oxides (MMO) which has strong base active sites (O^{2-}, OH^-). This property makes hydrotalcite very effective for various chemical reactions involving proton transfer mechanisms or acid–base reactions, such as transesterification of vegetable oil into biodiesel, aldol condensation reactions, isomerization reactions, and reforming of carbon dioxide gas. HT has wide applications such as adsorbent, medicine and catalyst because it has good ion exchange properties and is resistant to high temperatures. Furthermore, its porous structure and ability to evenly disperse metals make hydrotalcite ideal as a support for active metals (e.g., Ni, Co, or Cu) in hydrogenation and hydrocracking reactions (Duan *et al*., 2022).

HT as a catalyst is currently attracting considerable interest. HT as a heterogeneous catalyst is particularly attractive because it is easy to separate and resistant to high temperatures. However, because the pore size and surface area are relatively

* Corresponding author
Email: muhammad.al.muttaqii@brin.go.id (M. Al Muttaqii)

https://doi.org/10.61435/ijred.2026.61972
ISSN: 2252-4940/© 2026.The Author(s). Published by CBIORE

Table 1
Previous research on hydrotalcite as a catalyst

No.	Catalyst	Aplication	References
1	Ni–Al hydrotalcite	Methanation	(Zeng, Yao, Wang, & Gao, 2025)
2	Cu/Ni hydrotalcite	Hydrogenation	(Gupta & Kantam, 2018)
3	Hydrotalcite-Derived Metal	Catalytic Upgrading	(Hui, Zhuohua, Tong, & Yuan, 2022)
4	Ca riched Hydrotalcite	Transesterification	(Çakırca & Akın, 2021)
5	Hydrotalcite	Deoxygenation	(Prabhakara, Bramer, & Brem, 2022)
6	Ni/Al hydrotalcite	Fast Pyrolysis	(Yang *et al*., 2024)
7	Ni-V/HTc	Hydrocracking	This study

moderate, it can cause pore blockage by reactants and coke. (Di *et al* 2025). Catalytic activity can be improved with modifications to the HT surface are necessary. One approach is impregnation with metal to increase its acidity and active sites. Some commonly used metals are Zn, Cu, Al, Cs, K, Ni and Co (Faria *et al.*, 2022; Kumar *et al*., 2024; Lin *et al*., 2021). Metal impregnation is also commonly performed using a bifunctional system, impregnating two metals simultaneously. Bifunctional metals are useful for increasing catalyst stability, surface area, and acid sites. The use of bimetals can increase liquid production and enhance isomerization and aromatization (Adany *et al.,* 2025; Al Muttaqii *et al*., 2025a). Nickel offers the advantages of low cost, high deoxygenation and hydrogenation activity, and selectivity toward hydrocarbons (Aziz *et al*., 2023). Vanadium, on the other hand, has excellent stability at high temperatures and is selective toward aromatic compounds, making it excellent for hydrocarbon cracking (Zhou *et al* 2025).

Hartati *et al*., (2025) reported that the effect of 10% Ni impregnation on the Ca/ZSM-5 catalyst resulted in higher catalytic activity, reaching a conversion of 96.65%. The resulting selectivity increased from 47.7% for Z11 to 66.6% for Z11-Ni10 towards C15-C17. This indicates that nickel acts as an additional active site for DO and inhibits the secondary cracking reaction. In addition, the use of a Ni/H-ZSM-5 catalyst for the conversion of palmitic acid to n-alkanes achieved 86.17% conversion and 76.31% selectivity. Nickel is the most widely used metal for deoxygenation reactions because it offers high performance at relatively low cost compared to noble metals (Hongloi *et al* 2022; Hongloi *et al,* 2019; Sriatun *et al* 2020)

HT as a catalyst can be used in several catalytic reactions, one of which is the hydrocracking reaction to produce biofuel. Many previous studies have used HT as a catalyst in biodiesel, methanation and hydrogen production (Table 1). For example, (Çakırca & Akın, 2021) conducted a transesterification reaction of microalgae into biodiesel using HT as a catalyst. Several other studies have also conducted similar experiments using metal support (Cabrera *et al.*, 2025; Shrivastava *et al.*, 2023). In addition, several studies have used HT as a catalyst in the production of bio-oil from biomass (Guo *et al.*, 2023; Lu *et al.*, 2023). However, there has not been much research using HT as a catalyst for hydrocracking reactions, especially from feedstock using WCO. Hydrocracking is used to obtain shorter hydrocarbon chains with the aid of H_2 gas. Some feedstocks widely used in biofuel production include non-edible oils from plants such as *Cerbera manghaas, Reutealis trisperma, Jatropha curcas*, and others (Al Muttaqii *et al*., 2025a). Additionally, there are several potential feedstocks such as used oil, WCO, and asphalt (Ding *et al*., 2021; Jovita *et al*., 2024; Lam *et al*., 2017).

WCO is a very abundant and promising feedstock. It consists of saturated and unsaturated fatty acids, with the majority comprising approximately 63% unsaturated fatty acids (Rahman *et al*., 2025). Furthermore, Indonesia, with the largest oil palm plantations and the largest consumer of palm cooking oil in the world, produces 18.5% of WCO annually (Dwita *et al* 2024). High FFA content causes saponification (soap formation) when using homogeneous base catalysts such as NaOH or KOH, thereby reducing the efficiency of the transesterification reaction. Therefore, a heterogeneous catalyst that is stable, active, and resistant to FFA and water is needed to optimize the process of converting WCO into biofuel. Furthermore, WCO has the potential to serve as a feedstock for hydrocracking reactions into biofuels, both diesel and aviation fuel fractions (Azira *et al* 2024). Therefore, this study examined Ni-V metal impregnation on HTc with varying metal ratios and catalyst loading ratios. Furthermore, catalytic hydrocracking tests was conducted on WCO at 350°C.

2. Materials and methods

2.1 Materials

This study were used commercial hydrotalcite (Sigma-Aldrich, with SA=78,0 m^2/g), Aquadest, $Ni(NO_3)_2{\cdot}6H_2O$ (≥99.99%, Merck), V_2O_5 (≥98%, Merck) and Waste Cooking Oil (WCO).

2.2 Impregnation of Nickel-Vanadium Metal in Hydrotalcite

Modification was carried out by adding two metals, Nickel and Vanadium, to the hydrotalcite using a hydrothermal impregnation method (Fig. 1). Modification was carried out in stages, using Nickel and then Vanadium with varying metal loadings of 5 and 10% and metal ratios of 1:1 and 1:2, resulting in four variations for each type of hydrotalcite. A 10 mL $Ni(NO_3)_2{\cdot}6H_2O$ solution was prepared and then slowly added to the hydrotalcite in a beaker glass with stirring at room temperature for 60 minutes. After that, it was left overnight at room temperature. Next, adapting the research procedure of Utami et al. (2019) (Utami *et al.*, 2019), the mixture was put into a hydrothermal vessel and then used an oven temperature of 80°C for 4 h. The results obtained were dried at 110°C overnight. Then, with the same steps, this Ni/HTc solid was added with 10 mL of V_2O_5 solution in a beaker glass, until finally the NiV/HTc solid was obtained. The results were calcined at 550°C for 3 h and then reduced using a hydrogen gas flow at 300°C for 3 h. The results obtained are weighed, stored and labeled according to the modification conditions and type of support. Then, they were prepared for the characterization stage.

2.3. Characterization of the catalyst

The crystallinity of all samples catalysts were determined by using X-ray diffraction (XRD) with powder diffractometer (PHILIPS-binary X'Pert MPD, 30 mA, 40 kV) and the radiation

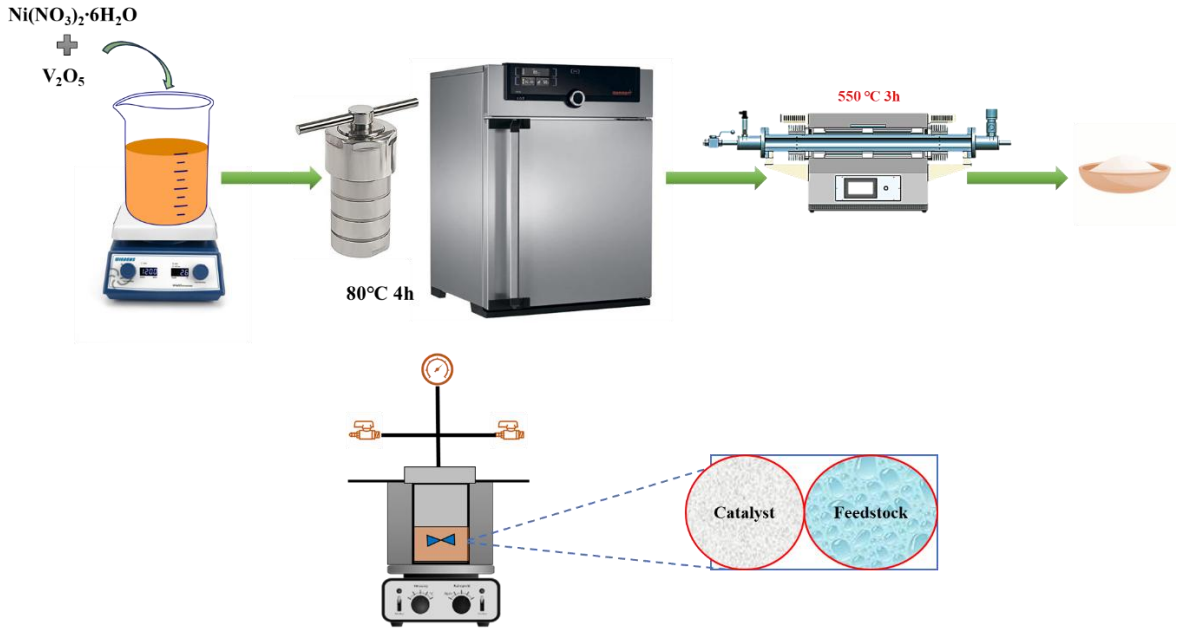

Fig. 1. Impregnation and catalytic activity illustration

of Cu-Ka ranging 2θ = 5°- 90°. The morphological and metal elemental distribution of all sample catalysts were characterized using Scanning Electron Microscopy-Energy Dispersive X-ray (SEM-EDX) Jeol JSM-IT200. The textural properties such as surface area and pore volume were determined using N2 adsorption–desorption of Quantachrome Touchwin v1.11 instrument. Quantachrome ASiQwin instrument was used to calculate the pore size distribution by BJH method.

2.4. Catalytic Activity

The catalytic activity testing process in this study was adapted from the methods used by Marlinda *et al.* (2022) (Marlinda *et al.*, 2022) and Al-Muttaqii et al. (2025) (Al Muttaqii *et al.*, 2025b) (Fig. 1). The process was carried out using a batch reactor equipped with a mechanical stirrer. A total of 15 mL of WCO (feedstock oil) and 0.5 g of catalyst were introduced into the reactor. The reactor was then tightly closed to prevent gas from escaping into the environment during the cracking reaction. H_2 gas was breathed into the reactor three times at a pressure of 15-25 barr. Gas was then injected at a pressure of 20 barr with a holding time of approximately 10 minutes to ensure stable pressure. The reaction was carried out for 2 h at 350°C with stirring. After the reaction time was reached, the reactor was allowed to reach room temperature. Next, the product is centrifuged to separate the liquid cracking product and the solid catalyst. The solid catalyst was dried, weighed, the results recorded, and stored with appropriate labels. Then, the liquid product is measured, stored in vials, labelled and prepared for the characterization stage using GC-MS to determine the composition of the cracking product and the data will be used to analyze the catalytic activity of the catalyst used. The composition of the liquid product was determined from equation (1) and the Gasoline, Kerosene and Gasoil fractions were determined using equation (2) based on the GC-MS results.

$$\%\text{Yield LC} = \frac{Peak\ area\ of\ compound}{Total\ liquid\ peak\ area}\ x\ 100\% \qquad (1)$$

$$\%\text{Yield Fraction} = \frac{Peak\ area\ of\ Fraction}{Total\ hydrocarbon\ peak\ area}\ x\ 100\% \qquad (2)$$

3. Results and discussion

3.1 Characterization of the catalyst

In the XRD analysis results for variations of commercial hydrotalcite shown in Fig. 2, the addition of nickel and vanadium metals does not change the structure of the hydrotalcite, but the greater the mass of the added metal will result in a decrease in the intensity of the diffraction peak in the 2θ = 10–40⁰ region which indicates a decrease in crystallinity and increases the possibility of a decrease in surface area (Du *et al.*, 2024). The decrease in intensity is caused by the metal filling the pores and surface of the catalyst and the occurrence of thermal stress during the impregnation process (Anggoro *et al*, 2016; Prameswari *et al*, 2023; Mohiuddin *et al*, 2018). Meanwhile, in the 2θ = 35–70⁰ region, there is a shift in the

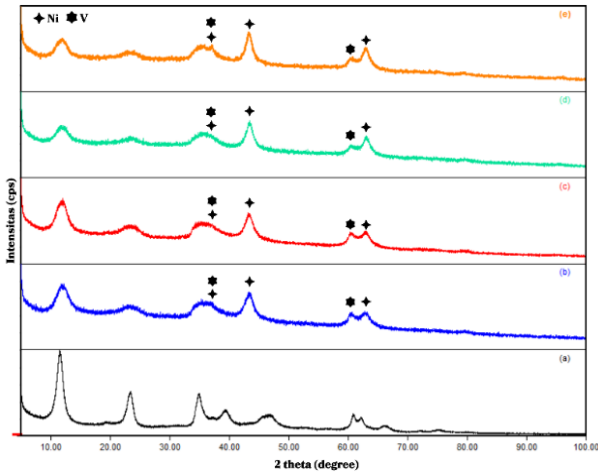

Fig. 2. XRD analysis results of (a) Commercial Hydrotalcite, (b) 5% Ni-V (1:1)/HTc, (c) 5% Ni-V (1:2)/HTc, (d) 10% Ni-V (1:1)/HTc, (e) 10% Ni-V (1:2)/HTc

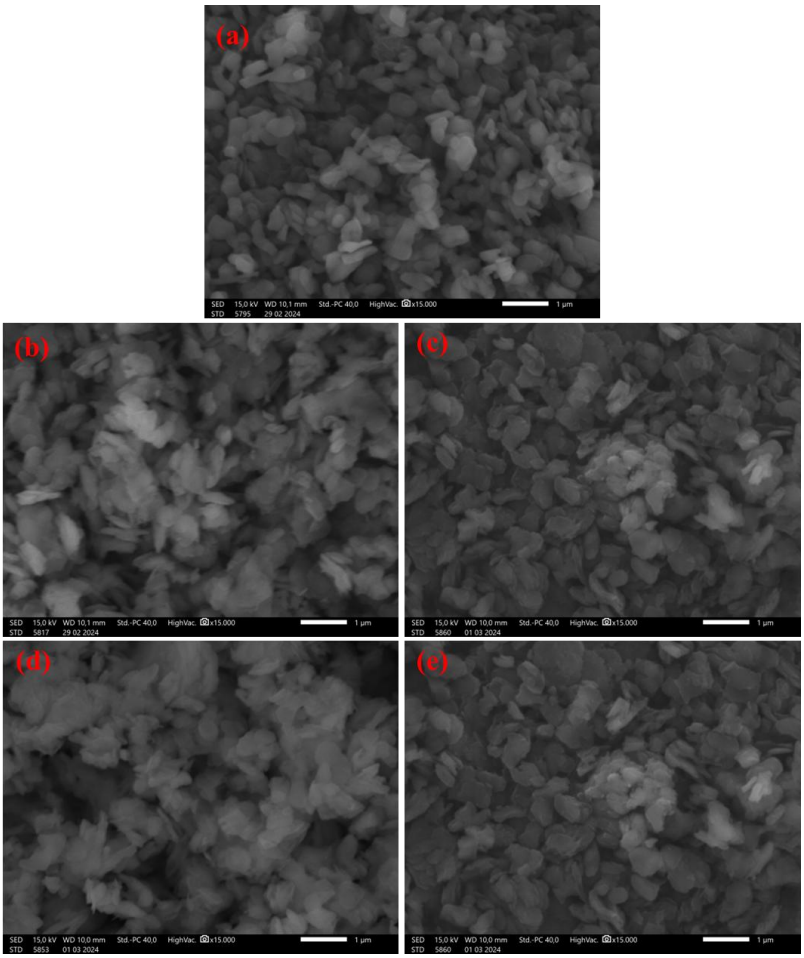

Fig. 3. SEM images of (a) HTc, modified with metal Ni-V: (b) 5% (1:1); (c) 5% (1:2); (d) 10% (1:1); (e) 10% (1:2)

characteristic peak of the hydrotalcite diffractogram (S. Wang, Zheng, & Lang, 2024). Nickel and vanadium metals were detected in the four modification variations, namely in the 2θ = 37.22º (Ni) and 37.35º (V) regions (Al Muttaqii *et al* 2021; Ma *et al* 2022). Furthermore, in the region 2θ = 43.58º, a high intensity characteristic peak belonging to nickel metal appeared and was detected in the region 2θ = 61.26º (V) and 63.07º (Ni). According to Paras *et al.* (2023) the crystallinity of the material can be determined by the sharpness of the diffraction peaks of the analyzed samples, a broad peak wave indicates an amorphous phase while samples with a high crystalline phase produce very sharp peaks.

SEM images of HTc (Fig. 3(a)) show a shape that is consistent with the characteristics of HT, namely the shape of the particles layered overlapping each other. In addition, the particle size of HTc is quite small with a scale of 1 μm indicating a particle size of hundreds of nanometers (Li *et al* 2026). The SEM results on HTc that have been impregnated with Ni and V metals show a similar morphological form, but with the presence of metal spread on the surface marked by white spots

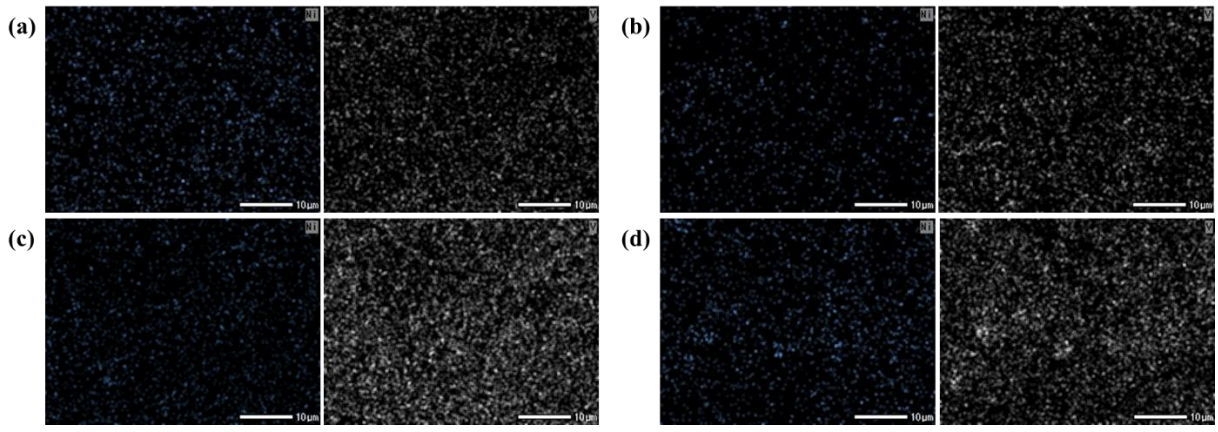

Fig. 4. Ni and V Mapping images of modified HTc with metal Ni-V (a) 5% (1:1); (b) 5% (1:2); (c) 10% (1:1); (d) 10% (1:2)

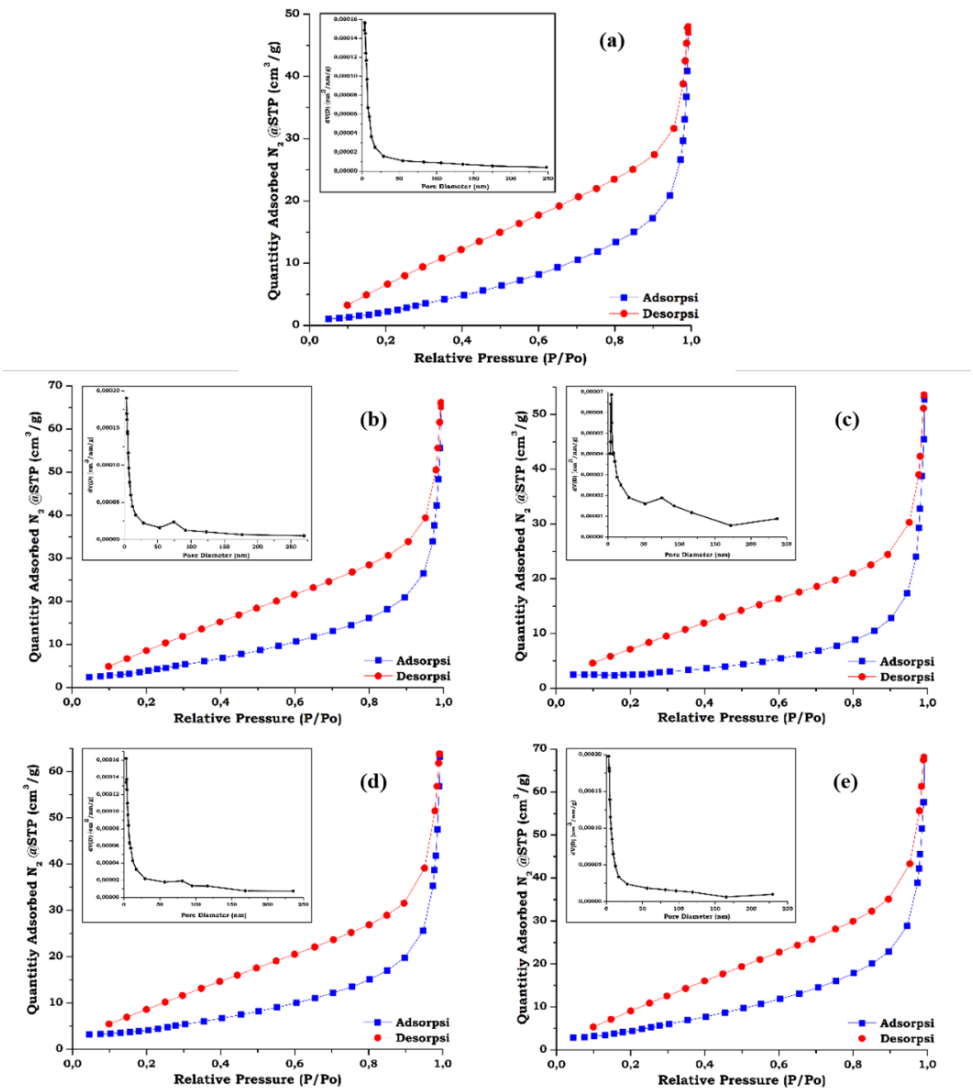

Fig. 5. N_2 adsorption-desorption isotherm graph and pore size distribution of (a) HTc, modified with metal Ni-V: (b) 5% (1:1); (c) 5% (1:2); (d) 10% (1:1); (e) 10% (1:2)

as shown in Fig. 3(b-e). The presence of metal also causes the particle size to increase because the metal is dispersed on the HT surface (Chen *et al.*, 2026). The dispersion of metals on the HTc surface is evidenced by the EDX mapping shown in Fig. 4. It can be seen that the metals are evenly distributed on the HTc surface. At 10% catalyst loading, more metal colors are seen, indicating that the amount of metal is greater on the HTc surface. Therefore, it can be concluded that Ni and V metals have been successfully impregnated on the HTc.

Fig. 5 shows convex shape of the BET model graph of the N_2 adsorption-desorption isotherm (P/P_0 = 0–1.0) demonstrates that all catalyst fall into the type IV adsorption isotherm, indicating a mesoporous structure (Parkash, 2020). The adsorption-desorption isotherm curves exhibit hysteresis loops at high relative pressures, but the desorption lines vary, indicating differences in the type and shape of the hysteresis loops associated with specific pore structures (Seekhiaw *et al* 2023). HTc and HTc impregnated by Ni-V are classified as having H3 hysteresis loops, representing the lamellar slit pore shape (Aziz *et al.*, 2024). Similar studies that synthesized and characterized materials resembling hydrotalcite or the LDH group found the same isotherm classification, namely the type IV N_2 adsorption-desorption isotherm with H3 hysteresis loops (Cui *et al.*, 2019; Lu *et al.*, 2019). Table 2 shows the indication of

Table 2
BET analysis results of HTc

Catalysts	Surface area (m^2/g)	Pore Volume (cm^3/g)	D_{pore} (nm)
HTc	13.884	0.072	20.998
5% Ni-V (1:1)/HTc	17.694	0.101	22.796
5% Ni-V (1:2)/HTc	8.671	0.081	37.642
10% Ni-V (1:1)/HTc	16.591	0.097	23.576
10% Ni-V (1:2) /HTc	19.915	0.104	21.070

metal development has an effect on the surface area, where in the modification of commercial hydrotalcite a significant increase is shown in the variation of 10% Ni-V (1:2)/HTc, namely 19.915 m^2/g. However, a decrease is shown in the variation of 5% Ni-V (1:2) /HTC, namely 8.671 m^2/g. Summa *et al.* (2021), stated that the increase in surface area occurs due to metal dispersion on the hydrotalcite surface, while the decrease can occur due to uneven metal dispersion so that the pores blockage occurs. The results of commercial hydrotalcite modification include mesoporous, with an average diameter in the interval of 21.070-37.642 nm. Based on research by Pan *et al.* (2021), the shape of the N_2 adsorption-desorption isotherm graph on all modifications of commercial hydrotalcite type IV which are included in the H3 hysteresis loops classification which represents the shape of slit-shaped pores.

3.2 Catalytic activity

Fig. 6 shows that the WCO feedstock has the largest composition of Dodecanoic acid, Palmitic acid, and Octadecenoic acid, namely 30.71, 19.80, and 19.35%. This indicates that WCO contains carboxylic acids with a hydrocarbon chain length range of C12-C18. As shown in previous studies also showed similar results (Alotaibi *et al.,* 2024; Chauhan *et al.*, 2025).

Analysis liquid product using GC-MS aims to determine the composition of the cracking product, the data of which would be used to determine the potential catalytic activity of the material used based on its conversion success. In this study, the hydrocracking reaction products were grouped into alkanes (paraffins, isoparaffins, cycloparaffins), alkenes/olefins, monocyclic aromatics, polycyclic aromatics (PAHs), carboxylic acids, esters, alcohols, and other compounds such as ketones, ethers, and amides, as presented in Table 2. Interpretation of the distribution of compound components resulting from the hydrocracking reaction with HTc is shown in Fig. 7. The results of the catalytic test reaction on commercial hydrotalcite can only convert 94.02% of the carboxylic acids in the used cooking oil feedstock into alkanes (3.63%) and alkenes (3.88%), as much as 87.60% of the carboxylic acids are not converted. In the modification of commercial hydrotalcite with a 5% Ni-V metal development ratio of 1:1, the conversion of carboxylic acids into alkanes (2.16%), alkenes (2.64%), polycyclic aromatic hydrocarbons (0.38%) with unconverted carboxylic acids of 88.57%. The increase in conversion occurs in the 5% Ni-V metal development ratio of 1:2 which leaves 81.28% of the carboxylate because it can produce alkanes (2.32%) and alkenes (5.83%). Then, the modification of commercial hydrotalcite with 10% Ni-V metal development at a ratio of 1:1 had the highest conversion of alkane products (4.93%), alkene (8.59%) and aromatic hydrocarbons (0.34%). However, other compounds were also produced with the highest percentage, namely 9.37% with a percentage of ester and alcohol products of 8.63%. While the modification with 10% Ni-V metal development at a ratio of 1:2 had a conversion of alkane products (4.38%) and alkene (11.13%), unconverted carboxylic acids of 67.81%, the reaction

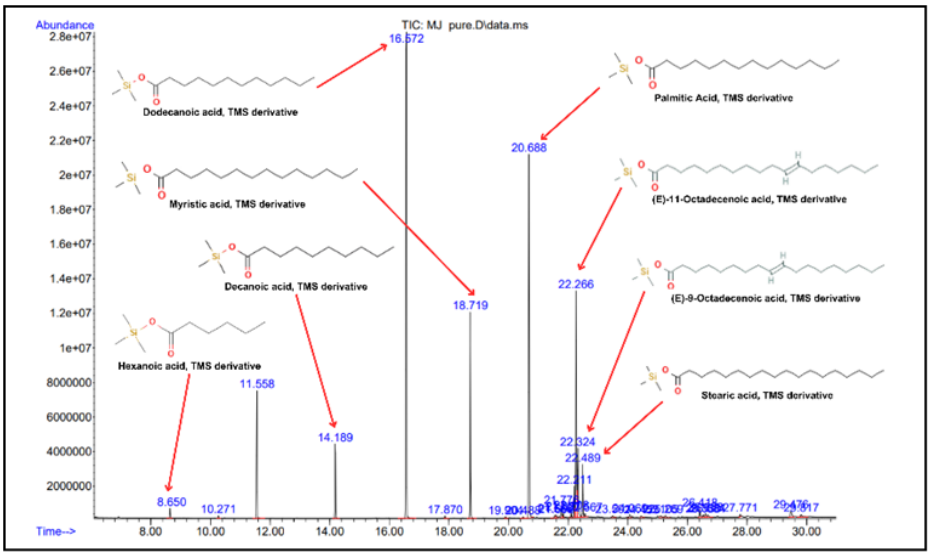

Fig. 6. GC-MS chromatogram of purified waste cooking oil

Table 3
Composition of the hydrocarbon compound group of liquid products

Composition	Catalyst				
	HTc	5% N-V (1:1)/HTc	5% N-V (1:2)/HTc	10% N-V (1:1)/HTc	10% N-V (1:2)/HTc
n-Paraffin	2.53	1.09	1.36	3.38	1.80
Iso-paraffin	0.00	0.26	0.31	0.00	0.37
Cyclo-paraffin	1.09	0.80	0.66	1.54	2.21
Aromatic	0.00	0.00	0.00	0.34	0.00
Olefin	3.88	2.64	5.83	8.59	11.13
Ester, Alcohol	2.00	2.98	3.42	8.63	9.21
Carboxylic acid	87.60	88.57	81.28	68.15	67.81
PAH	0.00	0.38	0.00	0.00	0.00
Etc.	2.89	3.28	7.14	9.37	7.47

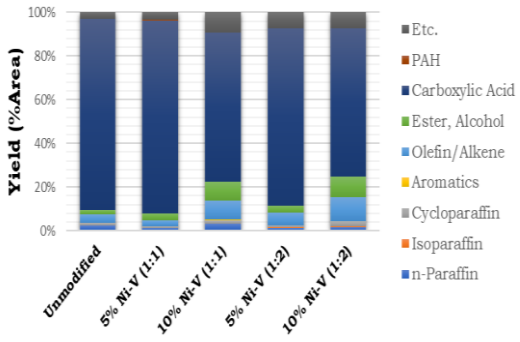

Fig. 7. Distribution of components of liquid product compound groups of hydrocracking reactions with HTc variations

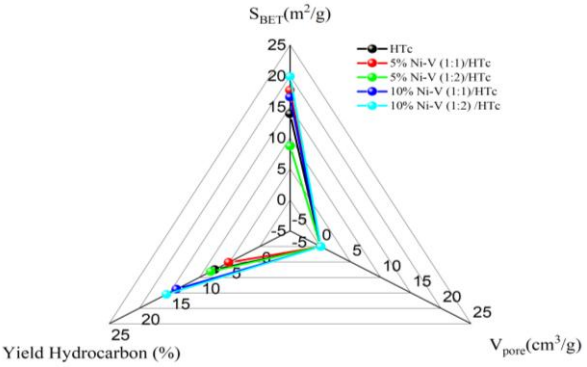

Fig. 9. Radar graph of the relationship between S_{BET}, pore volume and hydrocarbon yield

directed the conversion into other compounds (7.47%) and alcohol-ester (9.21%). The persistently high carboxylic acid content may be due to catalyst deactivation (Wang *et al.*, 2021). Furthermore, the relatively high carboxylic acid content may be due to an insufficiently high reaction temperature and an unsuitable catalyst (Banchapattanasakda *et al*, 2023; Satriadi *et al* 2022).

In this study, the alkane compounds, namely n-paraffin, isoparaffin, and cycloparaffin, produced by the hydrocracking reaction, were classified into three fractions. These three fractions are saturated hydrocarbons grouped based on the number of carbon atoms: gasoline (<C51-C9), kerosene (C10-C13), and gasoil (C14-C22<). The interpretation of the data from the product component fractions from hydrocracking is shown in Fig. 8, commercial hydrotalcite produces kerosene (0.83%) and gasoil (2.80%), the four variations in commercial hydrotalcite do not have any conversion into gasoline fractions. Then, at 5% Ni-V (1:1) HTc and 5% Ni-V (1:2) HTc, kerosene (0.40%) and gasoil were obtained at 1.76% and 1.92%, respectively. The highest product percentage was obtained at 10% Ni-V (1:1) HTc, namely kerosene (0.60%) and gasoil (4.33%), then at 5% Ni-V (1:2) HTc, kerosene (0.49%) and gasoil (3.89%). This is in accordance with previous research, most of which obtained biofuel results in the gasoil or long hydrocarbon chain range (Jovita *et al.*, 2024; Rashidi *et al.*, 2022).

The relatively low hydrocarbon yield (~15%) and the high proportion of residual carboxylic acids (~68%) indicate that the reaction did not proceed as a full hydrocracking process. Instead, the catalytic behavior is more representative of hydrogen-assisted upgrading involving partial deoxygenation and limited cracking (Santiko *et al* 2026). Hydrotalcite-derived

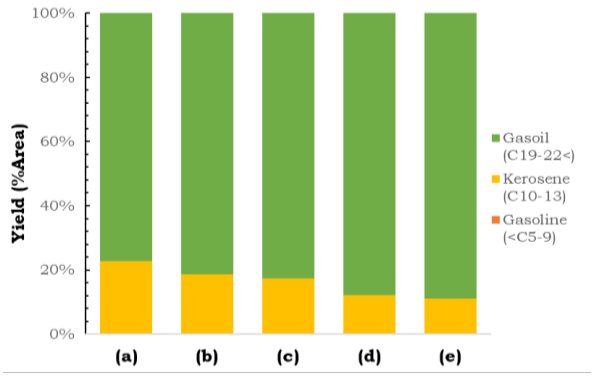

Fig. 8. Fractions of liquid product components from catalytic activity tests using: (a) HTc; (b) 5% Ni-V (1:1)/HTc; (c) 5% Ni-V (1:2)/HTc; (d) 10% Ni-V (1:1)/HTc; (e) 10% Ni-V (1:2)/HTc

catalysts are known to exhibit moderate acid–base properties, which favour reactions such as hydrogenation, ketonization, and decarboxylation rather than extensive C–C bond scission. In the present system, the Ni–V species likely promote partial hydrogenation and oxygen removal, while the insufficient density and strength of acidic sites limit deep hydrocracking activity. As a result, oxygenated intermediates, particularly carboxylic acids, remain dominant in the product mixture (Al Muttaqii *et al.,* 2024).

Fig. 9 shows the relationship between SBET, pore volume, and hydrocarbon yield. The higher the surface area, the higher the pore volume and hydrocarbon yield. In addition, the more metal impregnated causes the hydrocarbon yield to increase. This is associated with the increasing number of active sites of metal spread on the HTc surface. Then the ratio of Ni and V also affects the hydrocracking results and catalyst characteristics. The size of the NiO cation is larger compared to V_2O_5 which causes a 1:1 ratio to convert WCO into less hydrocarbons (Hartati *et al.*, 2025; Pan *et al.*, 2022). The +5 charge of Vanadium also makes the abundance of active sites and the smaller cation size causes the number of V_2O_5 cations to be much greater so that a 1:2 ratio obtains a greater hydrocarbon yield (Shen *et al.,* 2021).

4. Conclusion

Based on the conducted study, hydrotalcite-derived catalyst (HTc) materials were successfully synthesized and subsequently impregnated with bimetallic Ni–V at metal ratios of 1:1 and 1:2, with catalyst loadings of 5 wt% and 10 wt%. XRD analysis confirmed the successful incorporation of both metals onto the H Tc support. Characteristic diffraction peaks were observed in the 2θ range of 35–70° corresponding to HTc. Specific peaks at 2θ = 37.22° and 43.58° were attributed to NiO, while peaks at 2θ = 37.35° and 61.26° corresponded to V_2O_5 and metallic V, respectively. A peak at 63.07° further confirmed the presence of Ni species, indicating successful metal deposition without significant structural collapse of the HTc framework.

SEM analysis revealed a morphology consistent with typical hydrotalcite characteristics, showing layered structures with overlapping plate-like particles. The observed particle size was approximately 1 μm at the microscale, indicating primary particle dimensions in the range of several hundred nanometers. SEM-EDX elemental mapping demonstrated homogeneous dispersion of Ni and V across the HTc surface, suggesting effective impregnation and minimal metal agglomeration.

Nitrogen adsorption–desorption isotherm analysis indicated the formation of mesoporous structures, as evidenced by the

presence of hysteresis loops. Metal impregnation significantly enhanced the textural properties, increasing the surface area up to 19.915 m^2/g and enlarging the average pore diameter to 37.642 nm. Hydrocracking experiments using waste cooking oil (WCO) showed that the untreated reaction product contained a high proportion of carboxylic acids. However, the incorporation of Ni–V metals markedly improved catalytic performance, reducing the carboxylic acid content by up to 67.81%, demonstrating the effectiveness of the bimetallic HTc catalyst in promoting deoxygenation reactions.

Acknowledgment

The authors would like to express theirs thanks for financial support to the Deputy Facilitation Research and Innovation-National Research and Innovation Agency (DFRI-BRIN), and Indonesia Endowment Fund for Education Agency (LPDP). The authors acknowledge the facilities, scientific and technical support from Advanced Characterization Physics Laboratories Serpong, National Research and Innovation Agency through E-Layanan Sains, Badan Riset dan Inovasi Nasional (BRIN).

Author Contributions: L.M: writing—original draft, methodology, formal analysis, Resources, A.A.I.D: Investigation, visualization, formal analysis, S.P: writing—review and editing, M.P.M: writing—review and editing, resources, S.S: writing—review and editing, I.Y: project administration, A.A: Visualization, Validation, writing—review and editing, A.S.S: writing—review and editing, R.E.N: writing—review and editing, Visualization, M.A.M: Conceptualization, methodology, formal analysis, writing—original draft, supervision, resources. All authors have read and agreed to the published version of the manuscript.

Funding: This work was supported in part by the Research Organization for Nanotechnology and Materials – National Research and Innovation Agency (BRIN) research grant 2025. This work also carried out with financial from the PNBP Faculty of Science and Technology, with scheme Applied Research, University of Jambi, for the 2025 Fiscal Year.

Conflicts of Interest: The authors declare no conflict of interest.

References

Alotaibi, A., Naeem, M., Wali Khan, A., Farooq, I., Ud Din, M. & Saharun, M. S. (2024). Optimization and cost analysis evaluation studies of the biodiesel production from waste cooking oil using Na–Si/Ce-500 heterogeneous catalyst. *Biomass and Bioenergy*, *182*, 107078. https://doi.org/10.1016/j.biombioe.2024.107078

Adany, F., Priyanto, S., Mirzayanti, Y. W., Marbun, M. P., Zainul Furqon, M. I., Amin, A. K., … Al Muttaqii, M. (2025). γ- Al2O3-supported Cobalt and Zinc as heterogeneous catalyst for biodiesel production assisted by ultrasonic wave. *Vacuum*, *240*, 114502. https://doi.org/10.1016/j.vacuum.2025.114502

Al Muttaqii, M., Kurniawansyah, F., Prajitno, D. H., & Roesyadi, A. (2021). Hydrocracking process of coconut oil using Ni-Zn/HZSM-5 catalyst for hydrocarbon biofuel production. *Journal of Physics: Conference Series*, *1725*(1). https://doi.org/10.1088/1742-6596/1725/1/012008

Al Muttaqii, Muhammad, Marbun, M. P., Sudibyo, S., Aunillah, A., Pranowo, D., Hasanudin, H., … Bardant, T. B. (2024). Conversion of Sunan Candlenut Oil to Aromatic Hydrocarbons with Hydrocracking Process Over Nano-HZSM-5 Catalyst. *Bulletin of Chemical Reaction Engineering and Catalysis*, *19*(1), 141–148. https://doi.org/10.9767/bcrec.20116

Anggoro, D. D., Hidayati, N., Buchori, L., & Mundriyastutik, Y. (2016). Effect of Co and Mo Loading by Impregnation and Ion Exchange Methods on Morphological Properties of Zeolite Y Catalyst. *Bulletin of Chemical Reaction Engineering & Catalysis* 11(1), 75–83. https://doi.org/10.9767/bcrec.11.1.418.75-83

Azira, N., Razak, A., Taufiq-yap, Y. H., & Derawi, D. (2024). Catalytic deoxygenation of waste cooking oil for sustainable bio-jet fuel : A comparative study of Ni-Co / SBA-15 and Ni-Co / SBA-15-SH catalysts. *Journal of Analytical and Applied Pyrolysis*, *178*, 106369. https://doi.org/10.1016/j.jaap.2024.106369

Aziz, A., Andini Putri, B. G., Prasetyoko, D., Nugraha, R. E., Holilah, H., Bahruji, H., … Asikin-Mijan, N. (2023). Synthesis of mesoporous zeolite Y using Sapindus rarak extract as natural organic surfactant for deoxygenation of Reutealis trisperma oil to biofuel. *RSC Advances*, *13*(46), 32648–32659. https://doi.org/10.1039/d3ra05390c

Aziz, A., Nugraha, R. E., Holilah, H., Bahruji, H., Al Muttaqii, M., Suprapto, S., & Prasetyoko, D. (2024). Hydrothermal study of synthesis mesoporous NaP zeolite using Sapindus rarak extract as natural surfactant. *Inorganic Chemistry Communications*, *165* 112497. https://doi.org/10.1016/j.inoche.2024.112497

Banchapattanasakda, W., Asavatesanupap, C., & Santikunaporn, M. (2023). Conversion of Waste Cooking Oil into Bio-Fuel via Pyrolysis. *Molecules,* 1–18. https://doi.org/10.3390/molecules28083590.

Cabrera, D. A., Dora, M., Casados, A. S., Romero, A., Aída, G., & Alejandre, G. (2025). Assessment of Biodiesel Production from Ricinus Communis Oil over Based Zinc and Aluminum Hydrotalcites Modified with Calcium. *BioEnergy Research*. https://doi.org/10.1007/s12155-025-10853-9

Çakırca, E. E., & Akın, N. (2021). *S*tudy on heterogeneous catalysts from calcined Ca riched hydrotalcite like compounds for biodiesel production. *Sustainable Chemistry and Pharmacy, 20*. https://doi.org/10.1016/j.scp.2021.100378.

Chauhan, S. J., Devliya, B., Patel, B., Nagapara, J., Mevada, S., Solanki, H., & Patel, H. D. (2025). Biodiesel production from waste cooking oil using novel heterogenous CaO-MgO-ZnO-TiO2 nanoconjugate catalyst (CMZT-Nano Cat): A green approach towards renewable energy. *Biomass and Bioenergy*, *200*, 107985. https://doi.org/10.1016/j.biombioe.2025.107985

Chen, X., Sun, C., Ye, R., Zhang, Y., Li, C., Hui, K., … Kawi, S. (2026). Tri-synergistic catalytic mechanism of La-doped ternary hydrotalcite for low-temperature CO 2 hydrogenation. *Applied Catalysis B: Environment and Energy*, *382*, 125909. https://doi.org/10.1016/j.apcatb.2025.125909

Cui, C., Ma, J., Wang, Z., Liu, W., Liu, W., & Wang, L. (2019). High performance of mn-doped mg alox mixed oxides for low temperature nox storage and release. *Catalysts*, *9*(8). https://doi.org/10.3390/catal9080677

Di, G., Nolfi, V., Gallucci, K., Mucciante, V., & Rossi, L. (2025). Production of Green Diesel via the Ni/Al Mo Hydrotalcite Catalyzed Deoxygenation of Rapeseed Oil. *Molecules,* 1–23. https://doi.org/10.3390/molecules30081699.

Ding, Y., Shan, B., Cao, X., Liu, Y., Huang, M., & Tang, B. (2021). Development of bio oil and bio asphalt by hydrothermal liquefaction using lignocellulose. *Journal of Cleaner Production*, *288*, 125586. https://doi.org/10.1016/j.jclepro.2020.125586

Du, Y., Huang, C., Jiang, W., Yan, Q., Li, Y., & Chen, G. (2024). Preparation of surface modified nano-hydrotalcite and its applicaiton as a flow improver for crude oil. *Fuel*, *357*(PC), 130005. https://doi.org/10.1016/j.fuel.2023.130005

Duan, W., Li, G., Wang, Z., Wang, D., Yu, Q., & Zhan, Y. (2022). Highly efficient production of hydrotalcite-like compounds from blast furnace slag. *Applied Clay Science*, *219*(11), 106441. https://doi.org/10.1016/j.clay.2022.106441

Dwita, A., Nazri, E., Rahmayani, D., Tambun, R., & Benguerba, Y. (2024). Biodiesel production using waste cooking oil and Amberlite 62i as heterogeneous catalyst : Sustainability energy solution. *Case Studies in Chemical and Environmental Engineering*, *10*, 101011. https://doi.org/10.1016/j.cscee.2024.101011

Faria, A. C., Trujillano, R., Rives, V., Miguel, C. V., Rodrigues, A. E., & Madeira, L. M. (2022). Alkali metal (Na, Cs and K) promoted hydrotalcites for high temperature CO2 capture from flue gas in cyclic adsorption processes. *Chemical Engineering Journal*, *427*, 131502. https://doi.org/10.1016/j.cej.2021.131502

Guo, X., Hong, P., Yao, L., Liu, X., Jiang, Z., & Shi, B. (2023). Catalytic hydrogenation of lignin-derived aldehydes over bimetallic PdNi

/ hydrotalcite catalyst under mild conditions. *Fuel*, *353*, 129231. https://doi.org/10.1016/j.fuel.2023.129231

Gupta, S. S. R., & Kantam, M. L. (2018). Selective hydrogenation of levulinic acid into γ -valerolactone over Cu / Ni hydrotalcite-derived catalyst. *Catalysis Today*, *309*, 189–194. https://doi.org/10.1016/j.cattod.2017.08.007

Hartati, H., Bintang, P., Firda, D., Prasetyoko, D., Dwi, D., Bahruji, H., … Edra, R. (2025). Conversion of volcano mud and marble waste to Ni / Ca / ZSM-5 catalyst for bio-jet fuel production from waste cooking oil and the effect of Ni loading. *Fuel*, *400*, 135756. https://doi.org/10.1016/j.fuel.2025.135756

Hongloi, N., Prapainainar, P., & Prapainainar, C. (2022). Review of green diesel production from fatty acid deoxygenation over Ni-based catalysts. *Molecular Catalysis*, *523*, 111696. https://doi.org/10.1016/j.mcat.2021.111696

Hongloi, N., Prapainainar, P., Seubsai, A., & Sudsakorn, K. (2019). Nickel catalyst with different supports for green diesel production. *Energy*, *182*, 306–320. https://doi.org/10.1016/j.energy.2019.06.020

Hui, Z., Zhuohua, Z., Tong, S., & Yuan, Q. (2022). Recent Advances in the Catalytic Upgrading of Biomass Platform Chemicals Via Hydrotalcite - Derived Metal Catalysts. *Transactions of Tianjin University*, *28*(2), 89–111. https://doi.org/10.1007/s12209-021-00307-6

Jovita, S., Holilah, H., Khairunisa, N. N., Bahruji, H., Nugraha, R. E., Sholeha, N. A., … Prasetyoko, D. (2024). Mesoporous silica catalyst using Sapindus rarak extract as template for deoxygenation of waste cooking oil to biofuels. *Case Studies in Chemical and Environmental Engineering*, *10*. https://doi.org/10.1016/j.cscee.2024.100935

Kumar, A., Biswas, B., Kaur, R., Krishna, B. B., Park, Y. K., & Bhaskar, T. (2024). Hydrotalcite supported cobalt and tungsten catalysts for valorization of lignin into valuable phenolics. *Journal of Industrial and Engineering Chemistry*, *131*, 514–530. https://doi.org/10.1016/j.jiec.2023.10.057

Lam, S. S., Wan Mahari, W. A., Jusoh, A., Chong, C. T., Lee, C. L., & Chase, H. A. (2017). Pyrolysis using microwave absorbents as reaction bed: An improved approach to transform used frying oil into biofuel product with desirable properties. *Journal of Cleaner Production*, *147*, 263–272. https://doi.org/10.1016/j.jclepro.2017.01.085

Lauermannová, A. M., Paterová, I., Patera, J., Skrbek, K., Jankovský, O., & Bartůněk, V. (2020). Hydrotalcites in construction materials. *Applied Sciences (Switzerland)*, *10*(22), 1–13. https://doi.org/10.3390/app10227989

Li, K., Luo, H., Wu, J., Ouyang, D., & Tang, J. (2026). Preparation of novel magnetic hydrotalcite-based adsorbents and their synergistic adsorption of dye molecules and heavy metal ions : Response surface methodology analysis and adsorption mechanisms investigation. *Colloids and Surfaces A : Physicochemical and Engineering Aspects,* 728(8). https://doi.org/10.1016/j.colsurfa.2025.138519.

Lin, J., Hu, C., Xu, X., Shao, M., Hu, Y., & Ma, C. (2021). Investigation of Various Metals on Hydrotalcite-based Cu/Zn/Al Catalysts in Methanol Steam Reforming. *Chemical Engineering and Technology*, 44(6), 1121–1130. https://doi.org/10.1002/ceat.202000486

Lu, B., Zhuang, J., Du, J., Gu, F., Xu, G., Zhong, Z., … Su, F. (2019). Highly dispersed ni nanocatalysts derived from nimnal-hydrotalcites as high-performing catalyst for low-temperature syngas. *Catalysts*, *9*(3), 1–15. https://doi.org/10.3390/catal9030282

Lu, T., Sun, Y., Shi, M., Ding, D., Ma, Z., Pan, Y., … Sun, Y. (2023). Ni doped MgAl hydrotalcite catalyzed hydrothermal liquefaction of microalgae for low N , O bio-oil production. *Fuel*, *333*(P1), 126437. https://doi.org/10.1016/j.fuel.2022.126437

Ma, R., Du, Y., Liu, X., Liu, J., & Wu, X. (2022). Synthesis of a novel CoNiV mixed oxides from hydrotalcite precursor and its application for selective catalytic oxidation of slip ammonia. *Journal of the Energy Institute*, *102*, 327–336. https://doi.org/10.1016/j.joei.2022.04.004

Marlinda, L., Prajitno, D. H., Roesyadi, A., Gunardi, I., Mirzayanti, Y. W., Al Muttaqii, M., & Budianto, A. (2022). Biofuel from hydrocracking of Cerbera manghas oil over Ni-Zn/HZSM-5 catalyst. *Ecletica Quimica*, *47*(1), 17–39. https://doi.org/10.26850/1678-4618eqj.v47.1.2022.p17-39

Mohiuddin, E., Mdleleni, M. M., & Key, D. (2018). Catalytic cracking of naphtha : The effect of Fe and Cr impregnated ZSM - 5 on olefin selectivity. *Applied Petrochemical Research*, *8*(2), 119–129. https://doi.org/10.1007/s13203-018-0200-2

Muttaqii, Muhammad Al, Annas, D., Yati, I., Kurniawan, H. H., Ndruru, S. T. C. L., Priyanto, S., … Marlinda, L. (2025a). Molybdenum-lanthanum supported on nano-HZSM-5 as catalyst for hydroprocessing of Cerbera manghas oil. *Inorganic Chemistry Communications*, *173*, 113855. https://doi.org/10.1016/j.inoche.2024.113855

Muttaqii, Muhammad Al, Annas, D., Yati, I., Kurniawan, H. H., Ndruru, S. T. C. L., Priyanto, S., … Marlinda, L. (2025b). Molybdenum-lanthanum supported on nano-HZSM-5 as catalyst for hydroprocessing of Cerbera manghas oil. *Inorganic Chemistry Communications*, *173*, 113855. https://doi.org/10.1016/j.inoche.2024.113855

Pan, T., Ge, S., Yu, M., Ju, Y., Zhang, R., Wu, P., & Zhou, K. (2022). Synthesis and consequence of Zn modified ZSM-5 zeolite supported Ni catalyst for catalytic aromatization of olefin / paraffin. *Fuel*, *311*, 122629. https://doi.org/10.1016/j.fuel.2021.122629

Paras, Yadav, K., Kumar, P., Teja, D. R., Chakraborty, S., Chakraborty, M., … Hang, D. R. (2023). A Review on Low-Dimensional Nanomaterials: Nanofabrication, Characterization and Applications. *Nanomaterials*, *13*(1), 1–44. https://doi.org/10.3390/nano13010160

Parkash, A. (2020). Doping of Fe on room-temperature-synthesized CoNi layered double hydroxide as an excellent bifunctional catalyst in alkaline media. *Journal of the Iranian Chemical Society*, *17*(11), 2943–2956. https://doi.org/10.1007/s13738-020-01970-7

Prabhakara, H. M., Bramer, E. A., & Brem, G. (2022). Hydrotalcite as a deoxygenation catalyst in fast pyrolysis of biomass for the production of high quality bio-oil. *Journal of Analytical and Applied Pyrolysis*, *161*, 105431. https://doi.org/10.1016/j.jaap.2022.105431

Prameswari, J., Widayat, W., Buchori, L., Hadiyanto, H.(2023). Novel iron sand-derived α-Fe2O3/CaO2 bifunctional catalyst for waste cooking oil-based biodiesel production. *Environmental Science and Pollution Research,* 30 (44), 98832 - 98847. https://doi.org/10.1007/s11356-022-21942-z

Rahman, A., Oktaufik, M. A. M., Widi, T., Guntoro, I., Soedjati, D., Abbas, N., … Lomak, A. (2025). Current scenario and potential of waste cooking oil as a feedstock for biodiesel production in Indonesia : Life cycle sustainability assessment (LCSA) review. *Case Studies in Chemical and Environmental Engineering*, *11*, 101067. https://doi.org/10.1016/j.cscee.2024.101067

Rashidi, N. A., Mustapha, E., Theng, Y. Y., Razak, N. A. A., Bar, N. A., Baharudin, K. B., & Derawi, D. (2022). Advanced biofuels from waste cooking oil via solventless and hydrogen-free catalytic deoxygenation over mesostructured Ni-Co/SBA-15, Ni-Fe/SBA-15, and Co-Fe/SBA-15 catalysts. *Fuel*, *313*, 122695. https://doi.org/10.1016/j.fuel.2021.122695

Santiko, E. B., Fauziah, S., Priyanto, S., Yustinah, Y., & Marlinda, L. (2026). Nickel-Lanthanum Impregnated into Natural Zeolite as a Catalyst for Biofuel Production from Sunflower Oil via Hydrocracking Process. *Bulletin of Chemical Reaction Engineering & Catalysis* , *21*(1), 68–79. https://doi.org/10.9767/bcrec.20503

Satriadi, H., Pratiwi, I.Y., Khuriyah, M., Widayat, W., Hadiyanto, H., Prameswari, J.(2022) Geothermal solid waste derived Ni/Zeolite catalyst for waste cooking oil processing. *Chemosphere*, 286, 131618, https://doi.org/10.1016/j.chemosphere.2021.131618

Seekhiaw, P., Jantasee, S., Praserthdam, P., & Jongsomjit, B. (2023). Effect of Strontium Modification in Mg-Al Mixed Oxide Catalysts on Product Distribution toward Catalytic Reaction of Ethanol. *ACS Omega*, *8*(36), 32775–32783. https://doi.org/10.1021/acsomega.3c03752

Shen, Y., Pan, T., Wang, L., Ren, Z., Zhang, W., & Huo, F. (2021). Programmable Logic in Metal – Organic Frameworks for Catalysis. *Advanced Materials, 2007442*, 1–30. https://doi.org/10.1002/adma.202007442

Shrivastava, S., Prajapati, P., Srivastava, P., Lodhi, A. P. S., Kumar, D.,

Sharma, V., … Agarwal, D. D. (2023). Chemical transesterification of soybean oil as a feedstock for stable biodiesel and biolubricant production by using Zn Al hydrotalcites as a catalyst and perform tribological assessment. *Industrial Crops & Products*, *192*, 116002. https://doi.org/10.1016/j.indcrop.2022.116002

Sriatun, S., Susanto, H., Widayat, W., & Darmawan, A. (2020). Hydrocracking of Coconut Oil on the NiO/Silica-Rich Zeolite Synthesized Using a Quaternary Ammonium Surfactant. *Indonesian Journal of Chemistry, 21*(2), 361-375. https://doi.org/10.22146/ijc.55522

Utami, M., Trisunaryanti, W., Shida, K., Tsushida, M., Kawakita, H., Ohto, K., … Tominaga, M. (2019). Hydrothermal preparation of a platinum-loaded sulphated nanozirconia catalyst for the effective conversion of waste low density polyethylene into gasoline-range hydrocarbons. *RSC Advances*, *9*(71), 41392–41401.https:/doi.org/10.1039/c9ra08834b

Wang, S., Zheng, Y., & Lang, M. (2024). Preparation of Hydrotalcite/SBA-15 Composite Catalyst and its Application in the Synthesis of ε-Caprolactone. *Catalysis Letters*, *154*(11), 6094–6105. https://doi.org/10.1007/s10562-024-04763-2

Wang, Y., Sun, K., Zhang, S., Xu, L., Hu, G., & Hu, X. (2021). Steam reforming of alcohols and carboxylic acids: Importance of carboxyl and alcoholic hydroxyl groups on coke properties. *Journal of the Energy Institute*, *98*, 85–97. https://doi.org/10.1016/j.joei.2021.06.002

Yang, D., Huang, J., Hu, Z., Miao, Y., Wang, F., Zhang, Z., … Pittman, C. U. (2024). Catalytic conversion of lignin into monoaromatic hydrocarbons over a Ni / Al hydrotalcite-derived catalyst. *Fuel*, *357*(PC), 129982. https://doi.org/10.1016/j.fuel.2023.129982

Zeng, J., Yao, Y., Wang, F., & Gao, J. (2025). Enhanced CO 2 methanation through electronic modification of Ru to Ni in Ni – Al hydrotalcite-derived catalysts. *Green Energy & Environment, 10*, 1280–1294. https://doi.org/10.1016/j.gee.2024.12.006

Zhou, T., Zhang, H., & Shi, J. (2025). Mechanistic insights and optimization of lignin depolymerization into aromatic monomers using vanadium-modified Dawson-type polyoxometalates. *International Journal of Biological Macromolecules*, *299*, 139644. https://doi.org/10.1016/j.ijbiomac.2025.139644

© 2026. The Author(s). This article is an open access article distributed under the terms and conditions of the Creative Commons Attribution-ShareAlike 4.0 (CC BY-SA) International License (http://creativecommons.org/licenses/by-sa/4.0/)